

# Faraday patterns in two-dimensional dipolar Bose-Einstein condensates

R. Nath and L. Santos

*Institut für Theoretische Physik, Leibniz Universität Hannover, Appelstrasse 2, D-30167 Hannover, Germany*

(Received 24 February 2009; revised manuscript received 5 October 2009; published 29 March 2010)

We analyze the physics of Faraday patterns in dipolar Bose-Einstein condensates. Faraday patterns can be induced in Bose-Einstein condensates by a periodic modulation of the system nonlinearity. We show that these patterns are remarkably different in dipolar gases with a roton-maxon excitation spectrum. Whereas for nondipolar gases the pattern size decreases monotonously with the driving frequency, patterns in dipolar gases present, even for shallow roton minima, a highly nontrivial frequency dependence characterized by abrupt pattern size transitions, which are especially pronounced when the dipolar interaction is modulated. Faraday patterns constitute, hence, an excellent tool for revealing the onset of the roton minimum, a key feature of dipolar gases.

DOI: [10.1103/PhysRevA.81.033626](https://doi.org/10.1103/PhysRevA.81.033626)

PACS number(s): 03.75.Kk, 05.30.Jp

## I. INTRODUCTION

Pattern formation in driven systems constitutes a general phenomenon observed in disparate scenarios ranging from hydrodynamics and nonlinear optics to liquid crystals and chemical reactions [1]. A paradigmatic example of pattern formation is provided by the Faraday patterns (or waves), which in their original formulation [2] refer to standing waves arising through a parametric instability on the surface of a vertically oscillated fluid. The equivalent of Faraday patterns may be observed in Bose-Einstein condensates (BECs) by modulating the nonlinearity arising from the interatomic interactions [3], either by time-dependent Feshbach resonances [4] or by a time-dependent confinement [5]. The latter method has been recently used for realizing these patterns in BECs [6,7]. Faraday patterns offer important insights about elementary excitations in BECs since the pattern size is determined by the Bogoliubov mode resonant with half of the driving frequency. For typical BECs the energy of elementary excitations grows monotonously as a function of their corresponding momenta. As a result, the pattern size decreases monotonously with the driving frequency [8].

Recent experiments on atoms with large magnetic moments [9,10], polar molecules [11,12], spinor BECs [13], and optical lattices [14] are opening the rapidly developing area of dipolar gases. In these gases, the dipole-dipole interactions (DDIs) play a significant or even dominant role compared to the short-range interactions (SRIs). Dipolar BECs present a wealth of new physics [15–18] due to the long-range and anisotropic character of the DDI. A major difference between nondipolar and dipolar BECs is provided by the dispersion of elementary excitations, which, due to the momentum dependence of the DDI, may show a roton-maxon character [18] similar to that encountered in helium [19]. Sufficiently deep rotonlike minima may significantly influence the critical superfluid velocity [18] and the finite temperature BEC physics [20] and may even lead to instability [21].

The rotonlike minimum has not yet been observed experimentally, and it remains still an open question how to probe easily the onset of rotonization. In this article, we show that pattern formation is crucially modified in dipolar BECs with an, even shallow, roton minimum in the excitation spectrum. Remarkably, contrary to the case of nondipolar BECs, the first unstable mode does not necessarily determine the emerging

pattern, which may be dominated by harmonics of the driving frequency with energies close to the roton minimum. As a result of that and of the multivalued character of the roton-maxon spectrum, the pattern size presents a highly nontrivial dependence with the driving frequency characterized even for shallow roton minima by abrupt transitions in the pattern size. These transitions, which are especially pronounced for modulated DDI, may be employed to reveal easily the appearance of a roton minimum in experiments on dipolar BECs.

The article is structured as follows. In Sec. II we present the physical system and the effective 2D model analyzed. In Sec. III we discuss the rotonlike Bogoliubov excitations in a 2D dipolar BEC. In Sec. IV we study Faraday patterns in dipolar gases with modulated SRIs. Section V is devoted to the physics of Faraday patterns when the DDI is modulated. Finally, in Sec. VI we comment on possible experimental realizations and summarize our conclusions.

## II. MODEL

In the following we consider a BEC of  $N$  particles with mass  $m$  and electric dipole  $d$  (the results are equally valid for magnetic dipoles) oriented in the  $z$  direction by a sufficiently large external field. The dipoles interact via a dipole-dipole potential:  $V_d(\vec{r}) = d^2[1 - 3\cos^2(\theta)]/r^3$ , where  $\theta$  is the angle formed by the vector joining the interacting particles and the dipole orientation. We assume a strong harmonic confinement  $V(z) = m\omega_z^2 z^2/2$  along the  $z$  direction, whereas for simplicity of our discussion we consider no  $xy$  trapping. At sufficiently low temperatures the BEC wave function  $\Psi(\vec{r})$  is given by the nonlocal nonlinear Schrödinger equation (NLSE):

$$i\hbar \frac{\partial}{\partial t} \Psi(\vec{r}) = \left[ \hat{H}_0 + \int d^3 r' U(\vec{r} - \vec{r}') |\Psi(\vec{r}')|^2 \right] \Psi(\vec{r}), \quad (1)$$

where  $\hat{H}_0 = -\hbar^2 \nabla^2/2m + V(z)$  and  $U(\vec{r}) = g\delta(\vec{r}) + V_d(\vec{r} - \vec{r}')$ , with  $g = 4\pi\hbar^2 a/m$ , where  $a$  is the  $s$ -wave scattering length (we consider in the following  $a < 0$ ) and  $m$  the particle mass. Note that the DDI introduce a nonlocal nonlinearity in Eq. (1). If the chemical potential (introduced later in this article)  $\mu_{2d} \ll \hbar\omega_z$ , the system can be considered “frozen” into

the ground state  $\phi_0(z)$  of  $V$  and hence the BEC wave function factorizes as  $\Psi(\vec{r}) = \psi(\vec{\rho})\phi_0(z)$ . Employing this factorization, the convolution theorem, the Fourier transform of the dipole-potential and integrating over the  $z$  direction, we arrive at the 2D NLSE [22],

$$i\hbar \frac{\partial}{\partial t} \psi(\vec{\rho}) = \left[ -\frac{\hbar^2}{2m} \nabla^2 + g_{2D} |\psi(\vec{\rho})|^2 + \frac{4\pi}{3} \beta g_{2D} \int \frac{d^2k}{(2\pi)^2} e^{i\vec{k}\cdot\vec{\rho}} \tilde{n}(\vec{k}) h_{2D} \left( \frac{kl_z}{\sqrt{2}} \right) \right] \psi(\vec{\rho}), \quad (2)$$

where  $\vec{k}$  is the  $xy$  wave number,  $l_z \equiv \sqrt{\hbar/m\omega_z}$  is the oscillator length,  $g_{2D} \equiv g/\sqrt{2\pi}l_z$  is the 2D short-range coupling constant,  $\tilde{n}(\vec{k})$  is the Fourier transform of  $|\psi(\vec{\rho})|^2$ , and  $h_{2D}(\vec{k}) = 2 - 3\sqrt{\pi}k e^{k^2} \text{erfc}(k)$ , with  $\text{erfc}(k)$  the complementary error function. The parameter  $\beta = d^2/g$  characterizes the DDI strength compared to the SRI.

### III. BOGOLIUBOV SPECTRUM OF A 2D DIPOLAR BEC

The homogeneous solution of (2) is  $\psi(\vec{\rho}, t) = \sqrt{n_{2D}} \exp[-i\mu_{2D}t/\hbar]$ , with  $n_{2D}$  the 2D homogeneous density and  $\mu_{2D} = g_{2D}n_{2D}(1 + 8\pi\beta/3)$  the chemical potential. The elementary excitations of the homogeneous 2D BEC are plane waves with 2D wave number  $\vec{k}$  and dispersion [23]

$$\epsilon(k)^2 = T(k) \left\{ T(k) + 2g_{2D}n_{2D} \left[ 1 + \frac{4\pi\beta}{3} h_{2D} \left( \frac{kl_z}{\sqrt{2}} \right) \right] \right\}, \quad (3)$$

where  $T(k) = \hbar^2 k^2/2m$  is the kinetic energy. If  $\beta = 0$  and since  $a < 0$ , then  $\epsilon(k \rightarrow 0)^2 < 0$  and phonon instability occurs, followed by the well-known collapse for attractive short-range interacting BECs. This instability is prevented for sufficiently large DDI such that  $g + 8\pi d^2/3 > 0$ . At moderate  $d$  values, and due to the  $k$  dependence of the DDI ( $h_{2D}$  function),  $\epsilon(k)$  may develop a rotonlike minimum for intermediate  $k$  values (an example for typical experimental values in  $^{52}\text{Cr}$  is shown in Fig. 1). The excitation spectrum presents hence a maximum and a minimum (roton-maxon spectrum), constituting one of the most relevant novel features in dipolar gases. We show below that this rotonlike minimum

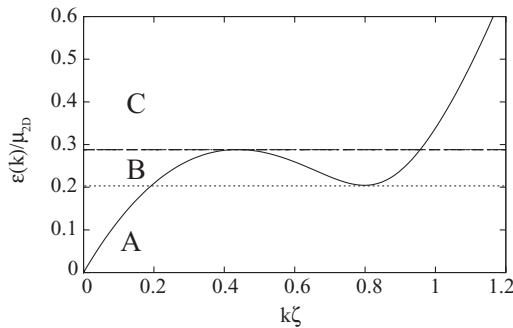


FIG. 1. Dispersion of a 2D homogeneous BEC of  $^{52}\text{Cr}$  with  $a = -0.54$  nm ( $\beta = -0.375$ ), a 3D density  $n_{2D}/\sqrt{2\pi}l_z = 10^{14}$  cm $^{-3}$ ,  $\hbar\omega_z = \mu_{2D}/2$ , and  $\zeta = \hbar/\sqrt{2m\mu_{2D}} = 0.59$   $\mu\text{m}$ . The excitation energies split into regimes A, B, and C (see text).

may be easily probed even for shallow rotonlike minima by modulating the system nonlinearity.

## IV. TIME MODULATION OF $s$ -WAVE SCATTERING LENGTH

### A. Mathieu equation and Floquet exponent

We consider a temporally periodic modulation of  $s$ -wave scattering length:  $a(t) = a_0[1 + 2\alpha \cos(2\omega t)]$  about its mean  $a_0$ , where  $\alpha$  is the modulation amplitude and  $2\omega$  is the driving frequency. The homogeneous 2D solution becomes  $\psi_H(\vec{\rho}, t) = \sqrt{n_{2D}} \exp\{-i[t + \frac{\gamma}{\omega} \sin(2\omega t)]\mu_{2D}/\hbar\}$ , with  $\gamma = \alpha/(1 + 8\pi\beta/3)$ . The driving may induce a dynamical instability breaking the translational symmetry of the homogeneous solution. This destabilization is best studied with an ansatz  $\psi(\vec{\rho}, t) = \psi_H(t)[1 + w(t) \cos(\vec{k} \cdot \vec{r})]$ , where  $w(t)$  is the complex perturbation amplitude. Inserting this ansatz into (2) and linearizing in  $w(t)$ , we obtain a Mathieu equation for  $u = \text{Re}(w)$ :

$$\frac{d^2u}{dt^2} + \frac{1}{\hbar^2} [\epsilon(k)^2 + 2b(\omega, k, \alpha)(\hbar\omega)^2 \cos(2\omega t)]u = 0, \quad (4)$$

with

$$b(\omega, k, \alpha) \equiv 2\alpha g_{2D} n_{2D} T(k)/(\hbar\omega)^2, \quad (5)$$

where  $g_{2D}$  is calculated from the mean  $a_0$ . Following the Floquet theorem [24], the solutions of (4) are of the form  $u(t) = c(t) \exp \sigma t$ , where  $c(t) = c(t + 2\pi/\omega)$  and  $\sigma(k, \omega, \alpha)$  is the so-called Floquet exponent. If  $\text{Re}(\sigma) > 0$ , the homogeneous BEC is dynamically unstable against the formation of Faraday patterns, whose typical wavelength is dominated by the most unstable mode [that with the largest  $\text{Re}(\sigma) > 0$ ]. For vanishing modulation the system becomes unstable at the parametric resonances  $\epsilon(k_n) = n\hbar\omega$ , where  $n = 1, 2, \dots$

### B. Nondipolar condensates

We discuss first for comparison the case of a nondipolar BEC ( $\beta = 0$ ) with  $g > 0$  (note that a nondipolar BEC with  $g < 0$  is always unstable under the conditions discussed in this article). In that case, the BEC presents a spectrum  $\epsilon(k)^2 = T(k)[T(k) + 2g_{2D}n_{2D}]$ , characterized by phononlike excitations at low  $k$  and single-particle excitations at large  $k$  with a smooth transition between them in the intermediate momentum of the order of  $1/\zeta$ , where  $\zeta = \hbar/\sqrt{2m\mu_{2D}}$  is the corresponding healing length. Hence, the spectrum of nondipolar BEC is constituted by a monotonously increasing nature. As discussed in [3,7], for any given driving frequency the most unstable mode is always provided by the first resonance  $\epsilon(k) = \hbar\omega$ , and hence  $k = \epsilon^{-1}(\hbar\omega)$  determines the typical inverse size of the Faraday pattern. Figure 2 shows the most unstable wave number as a function of the forcing frequency for the case of a nondipolar BEC. It is clear that the most unstable  $k$  increases with an increasing  $\omega$ , resulting in a monotonously decreasing pattern size, as shown in recent experiments [6,8]. From Fig. 2, it is interesting to note that the most unstable modes simply map the Bogoliubov spectrum of nondipolar BECs. In the following we show that the physics of Faraday patterns is remarkably much richer and involved in dipolar BECs.

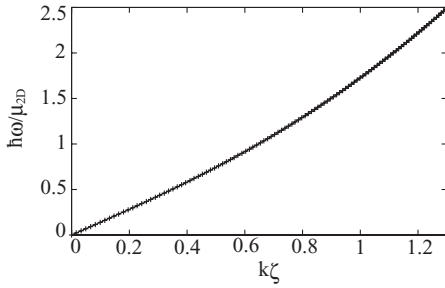


FIG. 2. Most unstable  $k$  as a function of forcing frequency  $\omega$  for modulated  $s$ -wave scattering length with  $\alpha = 0.2$  for a nondipolar BEC ( $\beta = 0$ ).

### C. Dipolar condensates

For  $\beta \neq 0$  and  $g > 0$ , for a 2D system the dispersion is similar to that of nondipolar BECs, and hence a monotonous wave number selection as that of Fig. 2 is expected. The situation is remarkably different when  $g < 0$ . As mentioned previously, for  $g < 0$  and intermediate  $d$  values  $\epsilon(k)$  the excitation spectrum shows a rotonlike minimum (with energy  $\hbar\omega_r$ ) and a maxon maximum ( $\hbar\omega_m$ ). Hence, as a function of the modulation frequency  $2\omega$  we may distinguish three driving regimes: (A)  $\omega < \omega_r$ , (B)  $\omega_r \leq \omega \leq \omega_m$ , and (C)  $\omega > \omega_m$  (see Fig. 1). The latter regime is relatively uninteresting, since, as for nondipolar BECs, the spectrum is univalued and the most unstable mode is provided by  $\epsilon(k) = \hbar\omega$  [white region in Fig. 3 (top)]. Hence, similar to the nondipolar case, the larger the driving frequency in regime C, the smaller the pattern size.

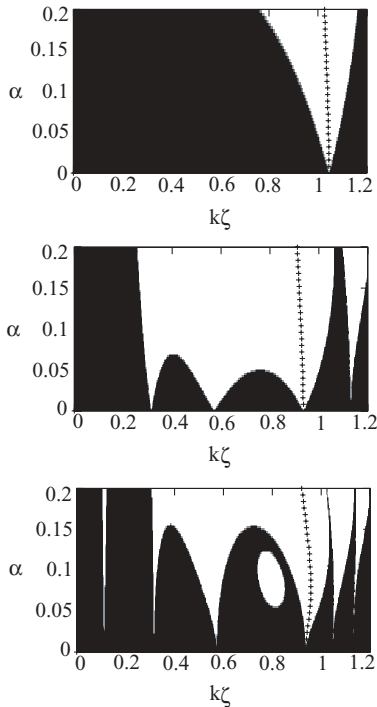


FIG. 3. Stability diagram (dark regions are stable) for the parameters of Fig. 1 as a function of  $\alpha$  and  $k$ . (Top)  $\hbar\omega/\mu = 0.4$  (regime C); (middle)  $\hbar\omega/\mu = 0.268$  (regime B); (bottom)  $\hbar\omega/\mu = 0.134$  (regime A). The most unstable modes are indicated by crosses.

Regime B on the contrary is multivalued, and the condition  $\epsilon(k) = \hbar\omega$  is satisfied by a triplet  $k_1^{(1)} < k_1^{(2)} < k_1^{(3)}$ . These three resonant momenta lead to three instability tongues for growing modulation amplitude  $\alpha$  [white regions in Fig. 3 (middle)]. However, these three wave numbers are not equally unstable. We may employ approximate expressions for the Floquet exponent for small  $b$  stemming from celestial mechanics (see [7,25] and references therein). The expression for  $\sigma$  up to fourth order in  $b(\omega, k, \alpha)$  can be obtained as

$$\sigma = \frac{i}{\pi} \arccos \left\{ \left[ 1 - \frac{b^4 \pi^2}{32n^2(1-n^2)^2} \right] \cos n\pi + \left[ \frac{-b^2 \pi}{4n(1-n^2)} + \frac{(15n^4 - 35n^2 + 8)b^4 \pi}{64n^3(1-n^2)^3(4-n^2)} \right] \sin n\pi \right\}. \quad (6)$$

Hence, for the lowest resonance  $\epsilon(k) = \hbar\omega$ , that is, for  $n = 1$ , we obtain

$$\sigma_1 \simeq b(\omega, k, \alpha)/2 \propto k^2/(\hbar\omega)^2. \quad (7)$$

It is clear that the most unstable mode in regime B is always given by the largest momentum among the triplet, and is  $k_1^{(3)}$ , which dominates the Faraday pattern formation and hence determines the pattern size. For regimes B and C the Faraday pattern is, as for nondipolar BECs, provided by  $\epsilon(k) = \hbar\omega$ . The situation is remarkably different for regime A. The latter is better understood by considering the ratio  $\sigma_2/\sigma_1$  between the Floquet exponents for the second [ $\epsilon(k) = 2\hbar\omega$ ] and the first [ $\epsilon(k) = \hbar\omega$ ] resonance condition. Again using Eq. (6), we obtain,

$$\sigma_2 = \frac{\sqrt{5}}{48} b^2. \quad (8)$$

Hence, the ratio between  $\sigma_1$  and  $\sigma_2$  can be obtained as

$$\frac{\sigma_2}{\sigma_1} = \frac{\sqrt{5}\alpha}{12(8\pi|\beta|/3-1)} \left( \frac{\mu_{2D}}{\hbar\omega} \right)^2 \zeta^2 \frac{[\epsilon^{-1}(2\hbar\omega)]^4}{[\epsilon^{-1}(\hbar\omega)]^2}. \quad (9)$$

Not surprisingly, the first resonance dominates for  $\alpha \rightarrow 0$ . However, contrary to the short-range interacting case, for  $\alpha$  surpassing a very small  $\omega$ -dependent critical  $\alpha$ , the situation changes completely. Figure 4 (top) depicts the ratio  $\sigma_2/\sigma_1$  as a function of  $\omega$  for a small  $\alpha = 0.04$ . Note that  $\sigma_2 < \sigma_1$  for  $\omega > \omega_r$  and, as expected, for regimes B and C the instability is dominated by the resonance  $\epsilon(k) = \hbar\omega$ . On the contrary, for  $\omega < \omega_r$ ,  $\sigma_2 > \sigma_1$ , even for such a small value of  $\alpha$ , and hence the lowest resonance is no longer the most unstable one.

This surprising result is a direct consequence of the dipole-induced roton-maxon dispersion, which allows for an anomalously large  $\epsilon^{-1}(2\hbar\omega)$  compared to  $\epsilon^{-1}(\hbar\omega)$ , which in turn, due to (9), results in  $\sigma_2 > \sigma_1$ . Note, however, that this effect cannot be directly extrapolated to other systems with a nonmonotonous dispersion relation, in particular to those presenting a nonmonotonous single-particle dispersion  $T(k)$  induced by an external periodic potential. This is, for example, the case of photonic crystals in nonlinear optics or condensates in particular optical lattices. Note that in general Eq. (9) becomes of the form  $\sigma_2/\sigma_1 \propto \alpha T(\epsilon^{-1}(2\omega))^2/\omega^2 T(\epsilon^{-1}(\omega))$ . Hence, the crucial condition  $\sigma_2 > \sigma_1$  demands an appropriate relation between  $T(k)$  and the many-body excitations

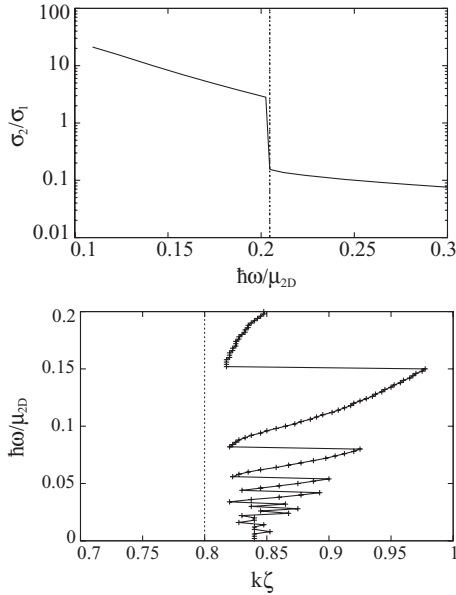


FIG. 4. Ratio between the Floquet exponent  $\sigma_1$  for  $\epsilon = \hbar\omega$  and  $\sigma_2$  for  $\epsilon = 2\hbar\omega$  (top). Most unstable  $k$  as a function of  $\omega$  in the regime A. We use the same parameters as for Fig. 1 and  $\alpha = 0.04$  (bottom). The dashed line indicates the roton frequency or momentum.

$\epsilon(k)$ . This point may be easily understood by considering a nondipolar BEC ( $d = 0$ ) with weak repulsive interactions  $g_{2D} > 0$ . If we consider momenta such that  $T(k) \gg g_{2D}n_{2D}$ , then  $\epsilon(k) \simeq T(k)$  and  $\sigma_2/\sigma_1 \propto \alpha/\omega$ . Hence, the first harmonic would remain the most unstable one regardless of whether  $T(k)$  is nonmonotonic.

Our numerical Floquet analysis shows indeed [see Fig. 4 (bottom)] that for  $\alpha > \alpha_{cr}$  (for the parameters of Figs. 3,  $\alpha_{cr} \simeq 0.027$ ) the most unstable mode for all driving frequencies within regime A is given by the largest momenta  $k$  compatible with the first harmonic  $\epsilon(k) = n\hbar\omega$  lying in regime B (or, if none, the first harmonic lying in regime C). This has important consequences for the wave-number selection as a function of the driving  $\omega$ , which, as shown in Fig. 4 (bottom), is remarkably different than that for the nondipolar case (see Fig. 2). The pattern size does not decrease monotonously with growing  $\omega$ , but on the contrary oscillates in the vicinity of the roton momentum, presenting abrupt changes of the pattern size at specific driving frequencies. These oscillations are the result of the subsequent destabilization of higher harmonics in regime B.

This distorted wave-number selection is directly mirrored into the spatial form of the corresponding patterns. We have studied the dynamical instability induced by the modulation and the emerging patterns by simulating Eq. (2) numerically with periodic boundary conditions and an overimposed random noise provided by a small random local phase ( $< 10^{-3}\pi$ ) on the homogeneous solution. Our direct numerical calculations are in excellent agreement with our Floquet analysis. Figure 5 (top left) depicts the case of a frequency  $\omega_r < \omega_0 < \omega_m$ , where as expected the Faraday pattern is indeed given by the largest resonant momentum. In Fig. 5 (top right) we consider  $\omega = \omega_0/2$ , which is within regime A [the corresponding stability diagram is depicted in

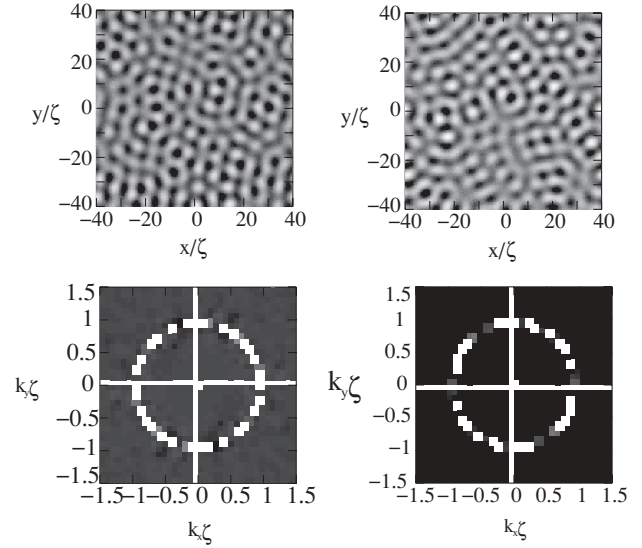


FIG. 5. Faraday patterns for  $\hbar\omega/\mu = 0.268$  at  $t = 40.6$  ms (top left) and  $\hbar\omega/\mu = 0.134$  at  $t = 93.2$  ms (top right) and the same parameters as in Fig. 1. Note that the pattern size is basically the same despite the very different driving frequencies. The corresponding Fourier transforms of the densities of the top figures are shown in the bottom panels. The white circle indicates the wave number of the corresponding pattern.

Fig. 4 (bottom)]. Strikingly, due to the discussed selection of higher harmonics, the Faraday pattern is basically the same as for a double driving frequency  $\omega_0$ . This quasi-insensitivity becomes quantitatively evident after Fourier transforming the density pattern (Fig. 5, bottom panels).

## V. TIME MODULATION OF DIPOLE-DIPOLE INTERACTION

In the previous section we considered the modulation of the  $s$ -wave scattering length  $a(t)$ . A dipolar BEC offers, however, an additional novel way of modifying the system nonlinearity by a time-dependent DDI. This may be achieved by modulating slightly the intensity of the polarizing field (e.g., the electric field orienting a polar molecule) or by introducing a slight precession of the direction of the external field (e.g., by additional transversal magnetic fields in the case of atomic dipoles). In the following we show that the Faraday patterns obtained by means of a modulated DDI differ very significantly from those obtained by modulating  $a(t)$ .

We consider a temporal modulation of the DDI  $d^2 = g\beta(t)$ , with  $\beta(t) = \bar{\beta}[1 + 2\alpha \cos(2\omega t)]$  about its mean value  $\bar{\beta}$ . Following a similar procedure as that discussed above for the case of modulated  $a(t)$ , we obtain the Mathieu equation for the real part of the perturbation amplitude  $u$ . This equation is of the same form as Eq. (4) but with

$$b(\omega, k, \alpha) = \frac{8\pi\alpha|\bar{\beta}g_{2D}|n_{2D}}{3(\hbar\omega)^2} T(k)h_{2D} \left( \frac{kl_z}{\sqrt{2}} \right). \quad (10)$$

The modified  $k$  dependence of  $b(\omega, k, \alpha)$  compared to Eq. (5), has crucial consequences for the formation of Faraday patterns. Similar to that described previously, we may employ the

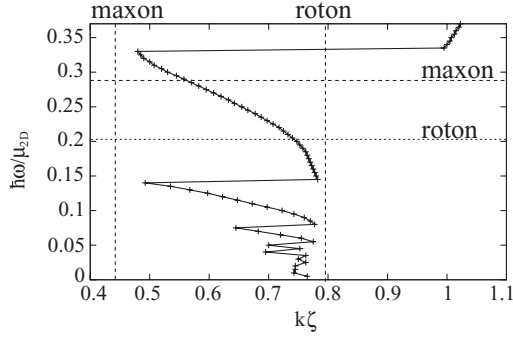


FIG. 6. Most unstable  $k$  as a function of  $\omega$  for modulated  $\beta(t)$ ,  $\alpha = 0.12$ , and the same parameters as for Fig. 1. We indicate the roton and maxon frequencies and momenta.

approximate expressions of the Floquet exponents [7,25]. Using Eq. (6), for the first resonance  $\epsilon(k) = \hbar\omega$ , we obtain

$$\sigma_1 \propto k^2 h_{2D} (kl_z / \sqrt{2}). \quad (11)$$

Note that the  $k$  dependence of  $\sigma_1$  is modified. Again, regime C is relatively uninteresting due to the univalued nature of the Bogoliubov spectrum. However, in regime B, the modified  $k$  dependence leads to a remarkably different selection rule for  $k$  values. Contrary to the case of modulated  $a(t)$ , it is the intermediate momentum  $k_1^{(2)}$  and not the largest one  $k_1^{(3)}$ , the one with the largest  $\sigma_1$  value, and hence the most unstable within regime B. This leads to a remarkably abrupt change in the Faraday pattern size in the vicinity of  $\omega_m$  [26]. In addition, and similar to the case of modulated  $a(t)$ , driving with  $\omega < \omega_r$  may be dominated by higher harmonics. Figure 6 shows the most unstable  $k$  as a function of  $\omega$  for a typical case of modulated  $\beta(t)$ . Note not only the aforementioned abrupt jump in the vicinity of  $\omega_m$  but also at other  $\omega$  values within regime A. As for the case of modulated  $a(t)$ , these jumps represent abrupt transitions in the Faraday pattern size, which are certainly much more marked than for those in the modulated  $a$  case. Figure 7 shows the abrupt change in the patterns for two driving frequencies right below and above the transition close to  $\omega_m$  [26].

We stress that these abrupt transitions in Faraday patterns in dipolar BEC are due to the rotonlike dispersion relation. Notably, this behavior is absent in dipolar BECs exhibiting a monotonous roton-free Bogoliubov spectrum. Hence, Faraday patterns can be used to probe even shallow rotonlike minima in dipolar gases. We mention at this point that alternative ideas have been proposed for revealing the presence of a rotonlike minimum, including the (experimentally rather involved)

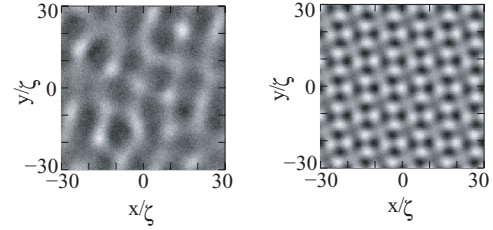


FIG. 7. Faraday patterns for  $\hbar\omega/\mu = 0.32$  at  $t = 97.3$  ms (left) and  $\hbar\omega/\mu = 0.34$  at  $t = 904.1$  ms (right) and the same parameters as in Fig. 6. Note that the pattern size is dramatically different despite the very similar driving frequencies.

analysis of the reduced critical superfluid velocity [18] and methods applicable for deep minima, such as the analysis of the modified finite temperature physics [20] or roton instability [20,21,27].

## VI. EXPERIMENTAL REALIZATION AND SUMMARY

In our calculations we have assumed for simplicity no trapping on the  $xy$  plane. A harmonic  $xy$  confinement (with frequency  $\omega_\perp$ ) leads to a finite momentum cutoff  $k_c = \sqrt{m\omega_\perp/\hbar}$ . In a good approximation all features in the excitation spectrum with momenta  $k \gg k_c$  are not affected by the inhomogeneous trapping. For typical roton momenta  $k\xi \simeq 0.5$  and  $\xi \simeq 0.6 \mu\text{m}$  in our figures,  $k \gg k_c$  demands for  $^{52}\text{Cr}$  a transversal frequency  $\omega_\perp < 130$  Hz, which can be considered a typical experimental condition. Finally, we stress that Faraday patterns are a transient phenomenon and that for the case discussed here ( $a < 0$ ) pattern formation is followed by collapse (and consequent violation of the two-dimensional condition).

In summary, pattern formation is largely modified in driven dipolar BECs in the presence of even shallow roton minima. Whereas in nondipolar BECs the Faraday pattern size decreases monotonously with the driving frequency  $2\omega$ , in dipolar BECs the patterns show a  $\omega$  dependence characterized by abrupt changes in the pattern size, which are especially remarkable when the dipole itself is modulated. Faraday patterns constitute, hence, an excellent tool for probing the onset of rotonization in ongoing experiments with dipolar condensates.

## ACKNOWLEDGMENTS

This work was supported by the DFG (SFB407, Cluster of Excellence QUEST) and the ESF (EUROQUASAR).

- [1] M. C. Cross and P. C. Hohenberg, Rev. Mod. Phys. **65**, 851 (1993).  
 [2] M. Faraday, Philos. Trans. R. Soc. London **121**, 299 (1831).  
 [3] K. Staliunas, S. Longhi, and G. J. de Valcárcel, Phys. Rev. Lett. **89**, 210406 (2002).

- [4] S. Inouye, M. R. Andrews, J. Stenger, H.-J. Miesner, D. M. Stamper-Kurn, and W. Ketterle, Nature (London) **392**, 151 (1998).  
 [5] M. Modugno, C. Tozzo, and F. Dalfovo, Phys. Rev. A **74**, 061601(R) (2006).

- [6] P. Engels, C. Atherton, and M. A. Hofer, Phys. Rev. Lett. **98**, 095301 (2007).
- [7] A. I. Nicolin, R. Carretero-González, and P. G. Kevrekidis, Phys. Rev. A **76**, 063609 (2007).
- [8] However, resonances with the transversal trapping may induce abrupt modifications of the created pattern [6, 7].
- [9] A. Griesmaier, J. Werner, S. Hensler, J. Stuhler, and T. Pfau, Phys. Rev. Lett. **94**, 160401 (2005).
- [10] Q. Beaufils, R. Chicireanu, T. Zanon, B. Laburthe-Tolra, E. Maréchal, L. Vernac, J.-C. Keller, and O. Gorceix, Phys. Rev. A **77**, 061601(R) (2008).
- [11] S. Ospelkaus, A. Peér, K.-K. Ni, J. J. Zirbel, B. Neyenhuis, S. Kotochigova, P. S. Julienne, J. Ye, and D. S. Jin, Nat. Phys. **04**, 622 (2008).
- [12] J. Deiglmayr, A. Grochola, M. Repp, K. Mörtlbauer, C. Glück, J. Lange, O. Dulieu, R. Wester, and M. Weidemüller, Phys. Rev. Lett. **101**, 133004 (2008).
- [13] M. Vengalattore, S. R. Leslie, J. Guzman, and D. M. Stamper-Kurn, Phys. Rev. Lett. **100**, 170403 (2008).
- [14] M. Fattori, G. Roati, B. Deissler, C. D’Errico, M. Zaccanti, M. Jona-Lasinio, L. Santos, M. Inguscio, and G. Modugno, Phys. Rev. Lett. **101**, 190405 (2008).
- [15] S. Yi and L. You, Phys. Rev. A **61**, 041604(R) (2000).
- [16] K. Góral, K. Rzążewski, and T. Pfau, Phys. Rev. A **61**, 051601(R) (2000).
- [17] L. Santos, G. V. Shlyapnikov, P. Zoller, and M. Lewenstein, Phys. Rev. Lett. **85**, 1791 (2000).
- [18] L. Santos, G. V. Shlyapnikov, and M. Lewenstein, Phys. Rev. Lett. **90**, 250403 (2003).
- [19] R. P. Feynman, Phys. Rev. **94**, 262 (1954).
- [20] D. W. Wang and E. Demler, e-print arXiv:0812.1838.
- [21] S. Komineas and N. R. Cooper, Phys. Rev. A **75**, 023623 (2007); S. Ronen, D. C. E. Bortolotti, and J. L. Bohn, Phys. Rev. Lett. **98**, 030406 (2007).
- [22] P. Pedri and L. Santos, Phys. Rev. Lett. **95**, 200404 (2005).
- [23] U. R. Fischer, Phys. Rev. A **73**, 031602(R) (2006).
- [24] P. M. Morse and H. Feshbach, *Methods of Theoretical Physics* (McGraw-Hill, New York, 1953).
- [25] A. Nicolin, Ph.D. thesis, Copenhagen, 2008.
- [26] For finite  $\alpha$ , the transitions slightly shift from their values at  $\alpha \simeq 0$ .
- [27] M. Klawunn and L. Santos, Phys. Rev. A **80**, 013611 (2009).